A Novel Class of Cysteine Protease Inhibitors: Solution Structure of Staphostatin A from *Staphylococcus aureus*†

Grzegorz Dubin,*,‡ Marcin Krajewski,§ Grzegorz Popowicz,§ Justyna Stec-Niemczyk,‡ Matthias Bochtler,||,⊥ Jan Potempa,‡ Adam Dubin,‡ and Tad A. Holak§

Faculty of Biotechnology, Jagiellonian University, ul. Gronostajowa 7, 30-387 Krakow, Poland, Max Planck Institute for Biochemistry, Am Klopferspitz 18A, D-82152 Martinsried, Germany, International Institute of Molecular and Cell Biology, ul. Trojdena 4, 02-109 Warszawa, Poland, and Max Planck Institute for Molecular Cell Biology and Genetics, Pfotenhauerstrasse 108, 01309 Dresden, Germany

Received July 23, 2003; Revised Manuscript Received September 22, 2003

ABSTRACT: A series of secreted proteases are included among the virulence factors documented for *Staphylococcus aureus*. In light of increasing antibiotic resistance of this dangerous human pathogen, these proteases are considered as suitable targets for the development of novel therapeutic strategies. The recent discovery of staphostatins, endogenous, highly specific, staphylococcal cysteine protease inhibitors, opened a possibility for structure-based design of low molecular weight analogues. Moreover, the crystal structure of staphostatin B revealed a distinct folding pattern and an unexpected, substrate-like binding mode. The solution structure of staphostatin A reported here confirms that staphostatins constitute a novel, distinct class of cysteine protease inhibitors. In addition, the structure knowledge-based mutagenesis studies shed light on individual structural features of staphostatin A, the inhibition mechanism, and the determinants of distinct specificity of staphostatins toward their target proteases.

Unlike other bacteria *Staphylococcus aureus* is able to colonize and infect virtually every tissue of the body and is therefore responsible for a wide variety of human diseases. In addition, increasing antibiotic resistance makes this versatile pathogen an emerging plaque of 21st century calling for new treatment strategies (*22*). In turn, the development of such strategies requires understanding of this bacteria physiology, which, although still very basic, already points to some interesting targets. Highly regulated expression of a multitude of extracellular and cell surface associated proteins has been demonstrated to be necessary for virulence (*1*). Among the staphylococcal secreted proteins, the proteases of three catalytic classes, including serine, cysteine, and metalloenzymes, have been indirectly associated with many different functions in the infection process. Unfortunately, the direct in vivo data remain scarce, and only recently information became available for a cysteine protease, staphopain B. *S. aureus* produces two distinct cysteine proteases, staphopains A and B. The latter protease is encoded in one operon (*ssp*)[1] with staphylococcal serine protease (SspA). The insertional inactivation of the *ssp* operon leads to a decrease in virulence in several animal infection models (*6*). In contrast, strains lacking only SspA remain virulent, at least in the mice skin abscess model (*31*). These results seem to point directly to an important role of staphopain B, but not SspA, in the infection process. Knockout studies of staphopain A, the second secretory cysteine protease of *S. aureus*, have not yet been reported. However, several lines of evidence, including protection of the rat skin from staphylococcal infection by P-cystatin α, an effective inhibitor of staphopain A elastolytic activity (*38*), seem to implicate this protease as an important virulence factor. In addition, a staphopain A homologue of *Staphylococcus epidermidis* was identified as an etiologic agent in perifollicular macular atrophy (*40*). Moreover, similar to other virulence factors, staphopains are tightly regulated. First, the protein production is controlled on the expression level by several regulatory loci, including *agr* and *sar*, the two major global virulence gene expression regulators (*25*). Second, the enzymes are secreted as inactive zymogens undergoing activation in a complicated network of interaction with other proteases.

Recently, increased interest in staphopains led to the discovery of specific, intracellular, protein inhibitors of these enzymes. The *s*taphylococcal *s*erine *p*rotease operon (*ssp*) encodes, besides SspA and staphopain B, a third protein designated SspC, a potent inhibitor of staphopain B. Similarly, in the *s*taphylococcal *c*ysteine *p*rotease operon (*scp*) an ORF downstream of the staphopain A gene (*scpA*) encodes staphostatin A, a specific inhibitor of this enzyme (*21*, *34*). Although the mentioned cysteine proteases share

† This work was supported in parts by Grants DFG SFB 469 from the German Science Foundation awarded to T.A.H., 6P04A 08320 from the State Committee for Scientific Research, Warsaw, Poland, awarded to A.D., and HPAW-CT-2002-80064 from the European Commission awarded to G.D. in the framework of The Archimedes Prize.

* Corresponding author. Phone: (+48-12) 252-6511. Fax: (+48-12) 252-6902. E-mail: gdubin@mol.uj.edu.pl.

‡ Jagiellonian University.

§ Max Planck Institute for Biochemistry.

|| International Institute of Molecular and Cell Biology.

⊥ Max Planck Institute for Molecular Cell Biology and Genetics.

[1] Abbreviations: *ssp*, staphylococcal serine protease operon; SspA, serine protease V8 protease; SspB, cysteine protease staphopain B; SspC, cysteine protease inhibitor staphostatin B; *scp*, staphylococcal cysteine protease operon; ScpA, cysteine protease staphopain A; P-cystatin α, phosphorylated cystatin α; hetNOE, heteronuclear nuclear Overhauser effect.

10.1021/bi035310j CCC: $25.00
Published on Web 11/01/2003

significant primary and high tertiary structure homology (*11*), their specific inhibitors show only limited similarities at the amino acid sequence level. The semblance allowed preliminary classification of the latter proteins into one class of cysteine protease inhibitors; however, staphostatin A does not inhibit staphopain B, and SspC is not active against ScpA (*34*). Moreover, the inhibitors do not inhibit any other tested cysteine proteases, although staphopains are not structurally distinct, having a papain-like fold (*11*, *16*).

Most protein inhibitors of cysteine peptidases described up to now are structurally related and therefore were grouped into one superfamily designated cystatins. These homologous proteins are further divided into three families on the basis of details of their molecular structure. The inhibitors belonging to the first two families are about 12 kDa and differ in the content of disulfide bridges. The proteins of family 1 lack the disulfide bonds contrary to those of family 2. The third family encompasses proteins of much larger molecular sizes, containing several copies of the cystatin domain as well as unrelated domains. Cystatins have been described from several higher animal species, but examples are also found in many lower organisms (*2*, *4*). Staphostatin amino acid sequences, however, are not similar to the sequences of cystatins or other known protease inhibitors. The recently determined structure of staphostatin B shows a fold completely unrelated to that of cystatins but similar to the fold of lipocalins and in particular triabin, a serine protease inhibitor and von Ebner protein, a cysteine protease inhibitor (*33*). Nevertheless, the inhibition mode of staphopain B by staphostatin B is unique (*11*). The latter, therefore, becomes the first member of a novel class of cysteine protease inhibitors, staphostatin A being a very probable follower.

With the growing body of evidence indicating staphylococcal cysteine proteases as virulence determinants it becomes apparent that this class of proteins would make a good target for the development of a novel antistaphylococcal therapy. Staphostatins with their unique specificity make a good platform for rational design of low molecular weight, specific inhibitors. Perusing this goal and with the interest in the novel class of cysteine protease inhibitors, we decided to structurally characterize staphostatin A. The resulting NMR structure, structure−function relationship mutagenesis studies, and comparison with the previously characterized staphostatin B are presented below.

MATERIALS AND METHODS

Mutagenesis and Protein Purification. All mutagenesis studies were performed with the site-directed mutagenesis kit (Stratagene) according to the manufacturer's instructions. The following primer pairs (listed and a reverse-complementary one) were used: for the introduction of the C16A mutation 5′-GTA TTG ATA AAT TCA AAG CTA ATT CAG AGG CTA AGT ATT ATC-3′; to mutate C55 into Ala and for the generation of the double C16, C55 to Ala mutant 5′-GTG TTC TGT ATT TAT ATA TTT GGC AAT GTA ATC AGA ATC GTC TG-3′; for the generation of the G98A mutant 5′-GAA CAC AGA AGC TTT AGC GAC TTC TCC TAG AAT GAC-3′ and 5′-CAA TTA TGA ACA CAG AAG CTA TTG GAA CTT CTC CTA GAA-3′ to produce L97I substitution. All plasmids were sequenced to confirm the generation of the desired mutations.

The wild-type inhibitor and all mutants were purified according to the procedure described by Rzychon et al. (*34*) with some modifications. The plasmids were transformed into BL21 Star (DE3)pLysS cells (Invitrogen). The bacteria were grown at 37 °C, 160 rpm, according to the needs either in LB, M9, or selective labeling media to the OD_{600nm} = 1.0. The temperature was lowered to 30 °C, and expression was induced with 1 mM IPTG when the OD_{600nm} reached 1.2. Cells were harvested by centrifugation after 3 h in the case of LB and M9 media or after 2 h when grown in the selective labeling media. All of the following steps were done at 4 °C unless indicated otherwise. Cells were resuspended in PBS and lysed by sonication. The debris was centrifuged out at 75000*g*, and the supernatant was recirculated overnight over glutathione−Sepharose 4B (Pharmacia). After extensive washing with PBS, followed by a short wash with 50 mM Tris-HCl, pH 8.0, the protein was eluted with 10 mM reduced glutathione in the same Tris buffer. To cleave the fusion GST tag, thrombin (Sigma, T-9681) was added (250 units/15 mg of fusion protein), and the mixture was dialyzed at room temperature for 72 h to a 20-fold excess of 50 mM Tris-HCl, pH 8.0, containing 2 mM reduced and 2 mM oxidized glutathione and 0.5 mM EDTA. The latter buffer favors cysteine oxidation (*32*), and the time scale was chosen to allow for complete cleavage and oxidation. When the fusion protein was eluted with reduced glutathione and cleaved in the elution buffer, without dialysis, a mixture of oxidized and reduced forms resulted. To obtain the inhibitor with fully reduced cysteine residues, elution and the following steps were omitted, and the cleavage was carried out on the column by recirculating 50 mM Tris-HCl, pH 8.0, containing thrombin (100 units/L of starting culture) over glutathione−Sepharose with the bound fusion protein. In either case gel filtration was used to recover the free inhibitor and to exchange the buffer to 140 mM NaCl, 2.7 mM KCl,10 mM Na_2HPO_4, 1.8 mM KH_2PO_4, and 0.05% NaN_3, pH 7.5 (staphostatin A slowly aggregates in low-salt buffers). The samples were subsequently concentrated to approximately 8 mg/mL (∼0.7 mM), and D_2O was added to 10% to allow for NMR measurements. The protein could be easily concentrated to more than 20 mg/mL and was stable for several hours; however, a heavy precipitate formed after a few days, the concentration in the supernatant remaining at about 8 mg/mL. The yield ranges from 7 mg/L from the LB medium to 11 mg/L from the media used for selective labeling.

Protease Purification. Staphopain A was purified from *S. aureus* strain V8 by a combination of procedures previously described by Arvidson et al. (*3*), Potempa et al. (*27*), and Dubin et al. (*8*) to obtain pure, serine protease SspA free preparations. All of the following steps were done at 4 °C. Overnight cultures were centrifuged to remove the cells, and the protease-containing supernatant was precipitated with ammonium sulfate to 80% saturation (561 g/L). After centrifugation the pellets were resuspended in 80 mL of buffer A (50 mM Tris-HCl, pH 7.5) per liter of culture, and the solution was dialyzed against a 20× excess of the same buffer overnight. Subsequently, the dialyzate was applied to the preswollen and equilibrated DE52 ion exchanger (Whatmann; 5 g dry weight/L of culture), and the flow-through was collected and applied to preequilibrated SP-Sepharose (Sigma; 10 mL/L of culture). After elution with 1 M NaCl

in buffer A, the protein was applied to thiopropyl-Sepharose (Amersham Biosciences; 0.5 g dry weight/L of initial culture) and following extensive washing with buffer A eluted with 20 mM DTT in the same buffer. After overnight dialysis to a large excess of buffer A the pure staphopain was concentrated to the desired volume, aliquoted, and frozen for long-term storage (the preparation is stable for at least half a year at −20 °C).

Inhibitor Activity Assays. To assess the inhibitory activity of the wild-type and mutant proteins, the purified inhibitors were preincubated with tested proteases (staphopain A or B) in equimolar amounts and in 10-fold excess of inhibitor in 0.5 mL of 50 mM sodium phosphate buffer, pH 7.4, containing 2 mM cysteine and 1 mM EDTA for 5 min in 37 °C. Azocoll (2 mg) (Calbiochem) was added, the reaction mixture was incubated for another 30 min and centrifuged, and the absorbance of the supernatant (containing the digested substrate) was measured at 520 nm.

NMR Spectroscopy. All NMR experiments were recorded at 27 °C on Bruker AMX500, DRX600, or DMX750 spectrometers equipped with triple resonance probe heads and pulsed-field gradient units. The sequence-specific assignment of ^{1}H, ^{15}N, $^{13}C^{\alpha}$, and $^{13}C^{\beta}$ resonances was accomplished with the use of HNCA (*15*, *19*) and CBCA(CO)NH (*14*, *43*) spectra of the uniformly $^{15}N/^{13}C/70\%$ D-labeled sample and $^{1}H-^{15}N$ HSQC (*23*) spectra of ^{15}N uniformly and ^{15}N Tyr, Lys, Val, Ile, Gly/Ser, Leu, and Phe selectively labeled samples. In addition, ^{15}N-edited 3D NOESY (*26*, *35*), 2D TOCSY (*7*), and 2D NOESY (*26*) in 10% D_2O/90% H_2O and 100% D_2O were used. HSQC, HNCA, and CBCA(CO)NH experiments were recorded with respectively 128, 64 × 64, and 64 × 64 increments in indirect dimensions, and linear prediction was used to double the numbers. NOESY planes of 720 × 4096 points were recorded. For all experiments zero filling was used prior to the Fourier transform. The HNHA experiment (*12*) was acquired to obtain the $^{3}J_{HN\alpha}$ coupling constants for the determination of torsion angle constraints. Furthermore, modified versions of $^{1}H-^{15}N$ hetNOE (*10*, *24*, *30*) and T_1 relaxation time experiments (*36*) were measured to investigate the polypeptide backbone flexibility. For $^{1}H-^{15}N$ hetNOE experiments, amide protons were presaturated with 120 deg pulses for 2.5 s prior to the experiment. To determine T_1, six $^{1}H-^{15}N$ planes (256 × 2048 points) were recorded in an interleaved manner, with relaxation delays of 12.4, 384.4, 756.4, 1128.4, 1500.4, and 12.4 ms, and peak heights were taken for further analysis. All spectra were processed with the XWinNMR software of Bruker. The data of the ^{1}H, ^{15}N, and ^{13}C chemical shifts and $^{3}J_{HN\alpha}$ coupling constants of staphostatin A have been deposited in the BioMagResBank under accession number 5810.

Assignment and Structure Calculation. Sparky software (*13*) was used for data handling and assignment. For structure calculations the simulated annealing function of the CNS package (*5*) and energy minimization functions of SPDBV were utilized. Molmol2k (*20*), SPDBV, and WebLab ViewerPro were used for visualization of calculated structures and for statistics generation.

NOE distance constraints for structure calculations were derived from 2D NOESY spectra in H_2O and D_2O and from the ^{15}N-edited NOESY spectrum. For the quantification of peak intensities peak heights were used, and three classes of NOEs were distinguished: 4 Å for weak, 3 Å for medium, and 2 Å for strong signals. The uncertainties of the distances were set to ±2, ±1, and ±1 Å, respectively, in preliminary calculations, and some were later tightened near the ideal values (±0.3 Å) in well-defined secondary structures. Pseudoatom corrections were added to the upper bounds where eligible (*42*). Several rounds of calculations were performed, repeatedly violated NOEs were rechecked and removed if proved wrong, and new constraints assigned on the basis of preliminary structures were included in the following repeats. For the final round of calculations distance constraints were supplemented with ϕ torsion angles constraints derived from the HNHA experiment (*41*). Structure calculations were performed using standard protocols for simulated annealing (*17*) without the preceding distance geometry step. During the last step 200 conformers were generated, and the 20 best representatives were chosen on the basis of total energy value. The final family of structures was deposited in the Protein Data Bank under accession number 1OH1.

RESULTS

Cysteine Oxidation State. Several experiments were carried out to establish the oxidation state and to determine the importance for the protein function of two cysteine residues of staphostatin A. In preliminary purification trials the thrombin cleavage of the staphostatin A−GST fusion protein was performed in the reduced glutathione-containing elution buffer after the glutathione−Sepharose purification step. The 1D proton NMR spectra of the inhibitor showed two NMR peaks from the HE1 proton of tryptophan. Since staphostatin A contains only one Trp residue, the result indicated the presence of two forms of the protein. In contrast, when the fusion protein was cleaved directly on the column (the recombinant protein had no contact with buffers containing glutathione), only a single peak, corresponding to one of the previously observed resonances, was present in 1D NMR spectra of fresh samples. With time, however, the intensity of the peak decreased, and the protein slowly converted to another form as observed by the appearance and increase of a peak corresponding to the second observed resonance. It was therefore assumed that the two inhibitor forms represent different oxidation states of cysteine residues. The use of glutathione in the elution buffer favored oxidation of cysteines, therefore speeding the process of conversion. In further experiments, to obtain a homogeneous, time-stable, single form of the inhibitor, a refolding buffer supporting the oxidation of cysteines was used as described in Materials and Methods. The recombinant protein obtained with this method did not react with Ellman's reagent, indicating fully oxidized cysteine residues (*9*). Mass spectrometry analysis showed that two cysteine residues of staphostatin A formed an intramolecular disulfide bridge and the samples were free of molecules with mixed disulfides containing glutathione molecules. Significantly, when assayed for activity against staphopain A, both forms (reduced or oxidized protein) readily inhibited the enzyme.

To further investigate the importance of cysteine residues for the inhibitory function of staphostatin A, site-directed mutagenesis was employed to generate C16A, C55A, and the double mutant where both cysteine residues were

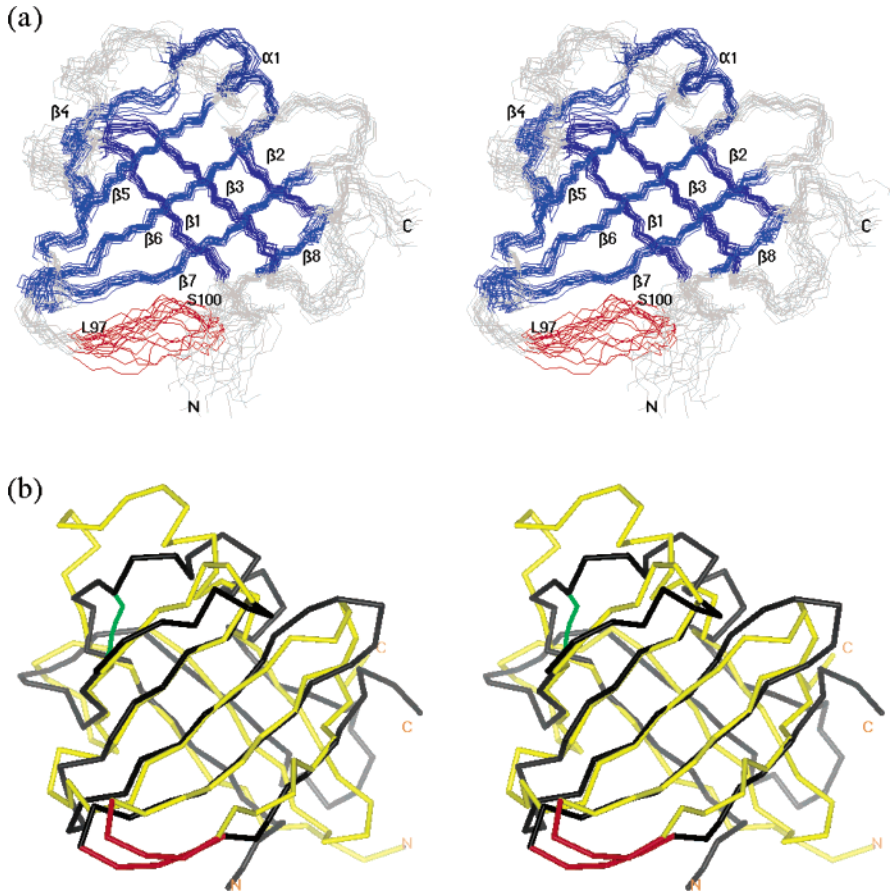

FIGURE 1: (a) Stereopair of overlays of the backbone (N, C^{α}, C′) atoms of the 20 final models of solution structure of staphostatin A. Well-defined secondary structures are in blue, and poorly defined regions are in gray. The protease active site occluding residues are colored in red. (b) Stereoview of the best backbone fit of a mean structure of staphostatin A (black; calculated for a family of 20 NMR structures, 1OH1) and of staphostatin B (yellow, 1NYC). C_{α} traces are shown. The protease active site occluding amino acids are highlighted in red. The disulfide bridge present in staphostatin A is colored green. The N and C termini are indicated.

exchanged to alanine residues. As suggested by the lack of effect of the cysteine residue's oxidation state on the inhibitory activity of staphostatins, all tested mutants also retained full activity against staphopain A.

Since neither the oxidation state of cysteine residues nor their replacement with alanine had any effect on the inhibitory activity, the wild-type protein with a disulfide bridge connecting residues C16 and C55 was used in further studies. The oxidized form was time stable, and its storage at 4 °C in PBS for several months did not influence inhibitory activity or affect NMR spectra, making it suitable for measurements. This was in contrast to the reduced form which slowly oxidized, resulting in the described doubling of the NMR resonance peaks.

Three-Dimensional Structure of Staphostatin A. The three-dimensional structure of staphostatin A was calculated from 564 approximate distance and 82 torsion angle constraints. A simulated annealing protocol, without a starting distance geometry step, was used to obtain a set of several hundred structures from which a family of the best 20 was selected as a representative of a solution structure of the inhibitor, using the criteria of total energy value. All selected structures fully satisfy the experimentally determined constraints, confirming that the final model corresponds well to the real structure of the protein in solution.

The staphostatin A polypeptide chain folds into a slightly deformed, eight-stranded β-barrel (Figure 1). Strands β4 through β8 form a standard antiparallel sheet while the N-terminus is best described as a ψ-loop motif (*18*). The connection between the first and second β-strands is extended and includes a short helix. The C-terminal-most strand is short, owing to an extended β7−β8 loop. The barrel-closing contacts between the N- and C-terminal parts consist of hydrogen bonds and a disulfide bridge. Thus, the overall fold of staphostatin A is identical to that of staphostatin B, providing unquestionable evidence that both proteins belong to the same, new class of cysteine protease inhibitors.

Inhibitor Reactive Site Mutants. In staphostatin B the region spanning amino acids residues 97−100 is responsible for the occlusion of the active site of protease. The unusual conformation of G98 ensures that the inhibitor, although bound in a substrate-like manner, remains uncleaved. Exchange of this residue to Ala or Arg, and probably to any other amino acid residue which, for steric reasons, cannot assume the conformation glycine does, converts the inhibitor into a substrate (*11*). As the structure of staphostatin A closely resembles that of staphostatin B, especially conserving the putative inhibitor reactive site sequence, the inhibitory mechanism of both proteins is most likely the same. To test this assumption, a G98A mutant of staphostatin A was constructed. As expected, the mutant no longer possessed inhibitory activity against staphopain A and was efficiently cleaved by the target protease (Figure 3b), demonstrating the substrate-like inhibitor binding mode.

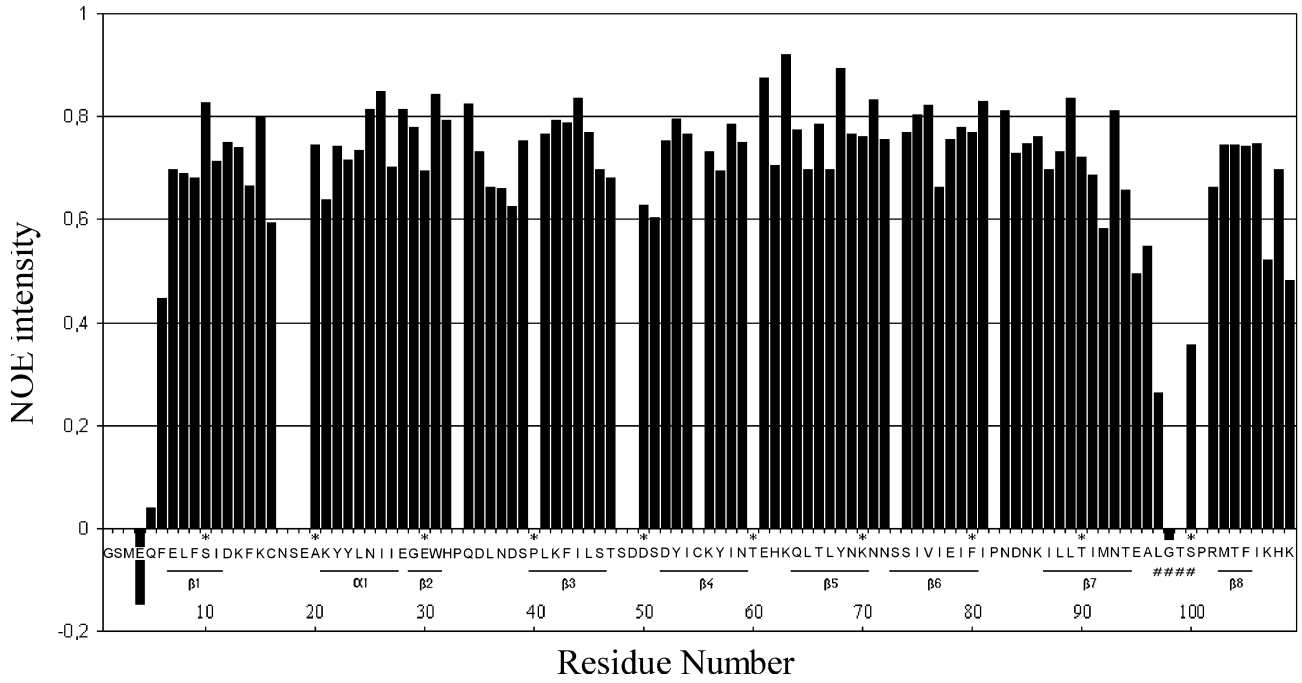

FIGURE 2: Steady-sate $\{^1H\}-^{15}N$ heteronuclear NOEs for the backbone amides of staphostatin A. (# indicates the reactive site loop residues).

Staphostatin B is exclusively specific for staphopain B, and staphostatin A inhibits only staphopain A without cross-inhibition. To test whether the binding loop is an exclusive specificity determinant of these inhibitors, the residue which is different in the two staphostatins in this region, the P2 positioned Leu-97 of staphostatin A, was exchanged to Ile, the corresponding residue of staphostatin B. The mutant retained its ability to inhibit staphopain A but showed no activity against staphopain B. This experiment shows clearly that the specificity of the inhibitors is determined outside the binding loop.

Molecular Motions in the Backbone of Staphostatin A. The intramolecular dynamics of staphostatin A was assessed by a heteronuclear, two-dimensional $^{15}N-\{^1H\}$ nuclear Overhauser effect (hetNOE) experiment (Figure 2) and T_1 relaxation studies (data not shown). The N-terminal part, spanning residues 1−6, was shown to be rather flexible, explaining its poorly defined and largely unstructured representation in the calculated structural model. This observation adds to the list of similarities between staphostatins since the corresponding residues in staphostatin B were shown to be unnecessary for the inhibition or protein folding (*33*). The C-terminal part does not show increased flexibility, which is also limited for the remaining residues, being in agreement with the inhibitor's tight β-barrel fold. Interestingly, the molecule possesses one more very flexible region spanning residues 95−101, which constitute the inhibitor reactive site (binding loop). Taken together, the ^{15}N NMR dynamics studies, crystallographic data for staphostatin B and the staphostatin B−staphopain B complex, and the results of protease binding studies presented below indicate that the inhibitor reactive site is not preformed and undergoes dynamic rearrangements (enabled by binding loop flexibility) upon protease binding to tightly fit into the enzyme active site cleft.

Protease Binding. As previously reported staphopain A binds staphostatin A in a 1:1 molar ratio (*34*). The complex is stable over extended incubation times; however, when assayed by SDS−PAGE a small fraction of the inhibitor is always cleaved, apparently directly upon binding, since the amount of the truncated part does not increase with time. To determine the processing site, MS analysis was performed, showing that staphostatin A is cleaved at the G98−T99 peptide bond, exactly as predicted by the substrate-like inhibitor binding model and by similarity to staphostatin B (Figure 3a).

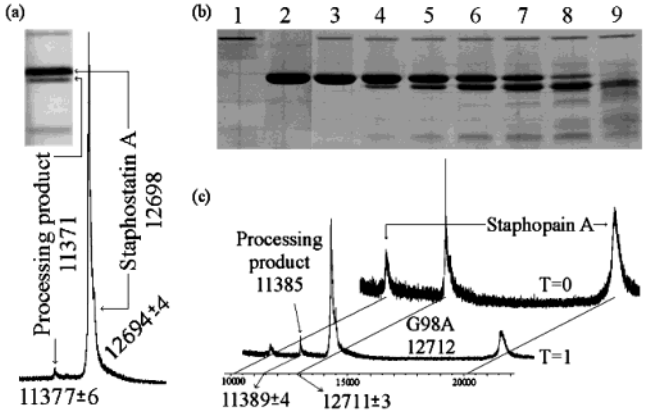

FIGURE 3: Staphostatin A (wt and G98A) protease binding studies. (a) MALDI-TOF trace of the staphopain A−staphostatin A complex after 72 h incubation at room temperature identifying the mass of the digestion product. SDS−PAGE of the sample is shown in the insert. (b) SDS−PAGE showing the effect of incubation of the G98A staphostatin A mutant with staphopain A (lanes: 1, protease; 2, G98A; 3, zero time; 4−9, samples withdrawn every 1 h). (c) MALDI-TOF traces of samples at zero and 1 h time from panel b, identifying the mass of the primary cleavage product.

When the G98A inhibitor reactive site mutant was incubated with staphopain A, instead of inhibiting the enzyme the protein was efficiently digested. The first cleavage was specific and occurred between residues A98 and T99 as determined by MS (Figure 3c). On longer incubation the truncated protein was digested into low molecular weight products.

DISCUSSION

Staphostatin A Cysteine Oxidation State. Two cysteine residues are present in the staphostatin A sequence, neither of which being necessary for inhibition since C16A, C53A, and a double cysteine to alanine mutant retain full inhibitory activity. Consistently, the single cysteine residue of staphostatin B is not necessary for inhibition, as elucidated from the protease−inhibitor complex structure and carboxymethylation studies (*11*, *34*). The inhibitors are produced in minute quantities by *S. aureus*, and it was impossible to determine the oxidation state of the natively produced staphostatin A. However, in vitro cysteine residues slowly oxidize, forming a disulfide bridge without any effect on inhibitory function. Since the oxidation results in doubling of peaks in the NMR spectra, to facilitate the measurements, cysteine residues were completely oxidized to disulfides prior to all experiments. Unfortunately, it was impossible to compare the binding kinetics of the isoforms and mutants utilized in this study as no good, synthetic substrate is available for staphopain A.

Preceding the NMR study a screening for crystallization conditions was performed, however without success, which seems justified by the inhomogeneity of the protein preparations used (*29*). Only with the NMR approach was it possible to visualize the isoforms and devise a purification procedure yielding homogeneous preparations, which allowed us to obtain crystals of staphostatin A; however, they did not diffract well enough for a promising structural analysis.

Staphostatins A and B Are Structurally Similar. The presented structure of staphostatin A (Figure 1a; see Supporting Information) shows the overall protein fold similar to that of staphostatin B (Figure 1b), confirming that apart from a low sequence similarity the proteins belong to the same, novel class of cysteine protease inhibitors. The distinct features of staphostatin A are the presence of a disulfide bridge and the two amino acid shorter connection between the N-terminal sheet and the helix. Moreover, the $\beta2-\beta3$ loop in staphostatin A diverges from the orientation found in staphostatin B due to a presence of two proline residues in the former and reflecting its solution flexibility compared to the highly packed crystal structure in case of the latter. Furthermore, the conformation of N-terminal residues also differs in the two proteins, this being consistent with the finding that these residues are unnecessary for binding and inhibition in staphostatin B. Apart from these small differences, the backbone fold of both proteins is identical.

Further Staphostatin Homologues. Two further staphostatin homologues have been identified in staphylococcal genomic sequences; however, to date no similar proteins have been found in any distant species (see Supporting Information). The *ecpB* gene of *S. epidermidis* is encoded together with a cysteine protease EcpA in one operon similar to the *scp* operon of *S. aureus*. Indeed, the sequences of corresponding proteins show higher homology to each other than to staphostatin B and staphopain B, respectively. Moreover, only staphostatin A inhibits EcpA while staphostatin B remains ineffective (EcpB has not been tested). This suggests that both staphostatins and staphopains may be divided into two groups on the basis of inhibition profiles and consistent with operon structure similarities. Further supporting the above suggestion, the last identified homologue of staphostatins, the *proD* gene of *Staphylococcus warnerii*, is encoded in an operon similar to *ssp* together with a serine protease ProM and a cysteine protease ProC. As expected, ProD shows higher homology to staphostatin B than to staphostatin A or EcpB. Likewise, ProC is more similar to staphopain B than to either staphopain A or EcpA. Unfortunately, neither ProD nor ProC have been isolated or tested.

Staphostatins A and B Use a Novel Inhibitory Mechanism. Cysteine protease inhibitors studied to date employ several diverse strategies for the regulation of their target proteases. Cystatins drift around the catalytic center, thus avoiding the cleavage. *I*nhibitors of *a*poptosis *p*rotein (IAP) family members target caspases directly spanning the substrate binding cleft however, in a direction opposite to natural substrates. The same is true for the zymogens of members of the papain family of cysteine proteases where an N-terminal profragment blocks a fully formed active site of the enzyme. Finally, viral proteins, p35 and CrmA, employ a so-called "mechanism-based inactivation" allowing forward binding and undergoing the initial step of cleavage but trapping the resulting thiol ester (acyl-enzyme) intermediate (reviewed in ref *37*). However, staphostatins fit none of these well-established patterns. Rather, the molecular basis for the regulation of staphopains resembles the "standard mechanism" employed by some serine protease inhibitors, which bind in a substrate-like manner forming a long-lived inhibitor−enzyme complex (*28*). Similarly, staphostatins occlude the active site of staphopains in a substrate-like manner, avoiding cleavage by the distinct disposition of the P1 glycine. The special, inhibitory conformation of the reactive site loop is not preformed in the free inhibitor (*11*, *33*), therefore calling for dynamic rearrangements upon binding. The heteronuclear NOE and T_1 relaxation time measurements for staphostatin A show the region spanning residues 95−101 to be highly mobile (Figure 2), confirming the dynamics of enzyme−inhibitor binding. It moreover may explain the structural divergence of this region observed in the two staphostatin B molecules present in the asymmetric crystal unit (*33*). The observed residual cleavage of the native inhibitor further supports such a dynamic mechanism. Thus, to our knowledge, staphostatins constitute the first examples of a novel, forward-binding, non-mechanism-based inhibitory strategy against cysteine proteases adapted by proteinaceous inhibitors.

Staphostatins Derive Specificity from Exosite Interactions. Though the structure of staphostatin A is reported here and structures of staphostatin B and the staphostatin B−staphopain B complex are also available (*11*, *33*), the mechanism of the extraordinary specificity of staphostatin A for staphopain A and staphostatin B for staphopain B without cross-inhibition or interaction with other cysteine proteases remains unresolved. To shed some light on this issue, we examined the inhibitory loop of staphostatins. In the region of contact with the active site of the protease only one residue differs between staphostatins A and B (respectively Leu and Ile at position 97). The difference between the side chains of those residues is not very pronounced; however, it could be enough to determine specificity. To test whether this would prove true, a L97I mutant of staphostatin A was constructed. The mutant, similarly to the wild-type staphostatin A, inhibited staphopain A and not staphopain B. These experimental data, together with suggestions elucidated from the enzyme−inhibitor complex structure (*11*), indicate that the inhibitory

loop by itself does not determine the unique specificity. Further mutagenesis studies are in progress to clarify that important issue.

CONCLUSIONS

Concluding, staphostatin A together with staphostatin B from *S. aureus* and two close homologues from *S. epidermidis* and *S. warnerii* constitute a new class of cysteine protease inhibitors distinct in the fold and the mechanism of action from any known inhibitors of these enzymes. Although the overall structural features link staphostatins to lipocalins and several β-barrel protease inhibitory/regulatory domains, the link is not supported by closer structural comparisons or the mechanism of action, making staphostatins the only members of the group.

The characterization of a novel class of cysteine protease inhibitors opens the way to interesting structure−function relationship studies since staphostatins, totally different from any known inhibitors of papain-like cysteine proteases, inhibit structurally similar enzymes by employing a method close to the standard mechanism utilized by some serine protease inhibitors. Moreover, structural characterization of staphostatins, together with the accumulating data on the importance of their target enzymes in pathogenesis, and currently available molecular biology and recombinant chemistry techniques provide a basis for the rational design of therapeutic inhibitors of staphopains for novel anti-staphylococcal treatments. Such a strategy was already proposed in 1990s; however, it could not have been developed due to the lack of knowledge on natural or synthetic staphopain inhibitors (*39*). Several issues, however, remain to be clarified, the most important being the elucidation of staphostatin specificity determination mechanisms.

ACKNOWLEDGMENT

The authors acknowledge Malgorzata Rzychon and Renata Filipek for sharing their results prior to publication, Jerzy Silberring and Tomasz Dylag for the MS analysis, and Artur Sabat for providing the staphostatin A expression plasmid.

SUPPORTING INFORMATION AVAILABLE

Amino acid sequence alignment of staphostatin A, staphostatin B, and their known homologues and ribbon diagrams of the staphostatin A structure. This material is available free of charge via the Internet at http://pubs.acs.org.

REFERENCES

1. Abdelnour, A., Arvidson, S., Bremell, T., Rydén, C., and Tarkowski, A. (1993) The accessory gene regulator (*agr*) controls *Staphylococcus aureus* virulence in a murine arthritis model, *Infect. Immun. 61*, 3879−3885.
2. Abrahamson, M. (1994) Cystatins in *Methods in Enzymology* (Barrett, A. J., Ed.) pp 685−700, Academic Press, San Diego.
3. Arvidson, S., Holme, T., and Lindholm, B. (1973) Studies on extracellular proteolytic enzymes form *Staphylococcus aureus*. I. Purification and characterization of one neutral and one alkaline protease, *Biochim. Biophys. Acta 302*, 135−148.
4. Barrett, A. J., Rawlings, N. D., Davies, M. E., Machleidt, W., Salvesen, G., and Turk, V. (1986) Cysteine proteinase inhibitors of the cystatin superfamily in *Proteinase inhibitors* (Barrett, A. J., and Salvesen, G., Eds.) pp 515−569, Elsevier, Amsterdam.
5. Brunger, A. T., Adams, P. D., Clore, G. M., Delano, W. L., Gros, P., Grosse-Kunstleve, R. W., Jiang, J. S., Kuszewski, J., Nilges, N., Pannu, N. S., Read, R. J., Rice, L. M., Simonson, T., and Warren G. L. (1998) Crystallography and NMR system: a new software suite for macromolecular structure determination, *Acta Crystallogr., Sect. D: Biol. Crystallogr. 54*, 905−921.
6. Coulter, S. N., Schwan, W. R., Ng, E. Y., Langhorne, M. H., Ritchie, H. D., Westbrock-Wadman, S., Hufnagle, W. O., Folger, K. R., Bayer, A. S., and Stover, C. K. (1998) *Staphylococcus aureus* genetic loci impacting growth and survival in multiple infection environments, *Mol. Microbiol. 30*, 393−404.
7. Dhalluin, C., Wierusyeski, J. M., and Lippens, G. (1996) An Improved Homonuclear TOCSY Experiment with Minimal Water Saturation, *J. Magn. Reson. B 111*, 168−179.
8. Dubin, G., Chmiel, D., Mak, P., Rakwalska, M., Rzychon, M., and Dubin, A. (2001) Molecular cloning and biochemical characterization of proteases form *Staphylococcus epidermidis*, *Biol. Chem. 382*, 1575−1582.
9. Ellman, G. L. (1959) Tissue sulfhydryl groups, *Arch. Biochem. Biophys. 82*, 70−77.
10. Farrow, N. A., Muhandiram, R., Singer, A. U., Pascal, S. M., Kay, C. M., Gish, G., Shoelson, S. E., Pawson, T., Forman-Kay, J. D., and Kay, L. E. (1994) Backbone Dynamics of a Free and a Phosphopeptide-Complexed Src Homology 2 Domain Studied by ^{15}N NMR Relaxation, *Biochemistry 33*, 5984−6003.
11. Filipek, R., Rzychon, M., Oleksy, A., Gruca, M., Dubin, A., Potempa, J. and Bochtler, M. (2003) The staphostatin-staphopian complex: a forward binding inhibitor in complex with its target cysteine protease, *J. Biol. Chem. 278*, 40959−40966.
12. Geerten, V. W., and Bax, A. (1993) Qualitative J Correlation: A New Approach for Measuring Homonuclear Three-Bond J(HNHA) Coupling Constants in ^{15}N-Enriched Proteins, *J. Am. Chem. Soc. 115*, 7772−7777.
13. Goddard, T. D., and Kneller, D. G., SPARKY 3, University of California, San Francisco.
14. Grzesiek, S., and Bax, A. (1992) Correlating Backbone Amide and Side Chain resonances in larger Proteins by Multiple Relayed Triple Resonance NMR, *J. Am. Chem. Soc. 114*, 6291−6293.
15. Grzesiek, S., and Bax, A. (1992) Improved 3D Triple-Resonance NMR Techniques Applied to a 31 kDa Protein, *J. Magn. Reson. 96*, 432−440.
16. Hofmann, B., Schomburg, D., and Hecht, H. J. (1993) Crystal structure of a thiol proteinase from *Staphylococcus aureus* V8 in the E-64 inhibitor complex, *Acta Crystallogr. 49* (Suppl.), 102.
17. Holak, T. A., Gondol, D., Otlewski, J., and Wilusz, T. (1989) Determination of the complete three-dimensional structure of the trypsin inhibitor from squash seeds in aqueous solution by nuclear magnetic resonance and a combination of distance geometry and dynamical simulated annealing, *J. Mol. Biol. 210*, 635−648.
18. Hutchinson, E. G., and Thornton, J. M. (1990) HERA−a program to draw schematic diagrams of protein secondary structures, *Proteins 8*, 203−212.
19. Kay, L., Ikura, M., Tschudin, R., and Bax, A. (1990) Three-Dimensional Triple-Resonance NMR Spectroscopy of Isotopically Enriched Proteins, *J. Magn. Reson. 89*, 496−514.
20. Koradi, R., Billeter, M., and Wüthrich, K. (1996) MOLMOL: a program for display and analysis of macromolecular structures, *J. Mol. Graphics 14*, 51−55.
21. Massimi, I., Park, E., Rice, K., Muller-Esterl, W., Sauder, D., and McGavin, M. J. (2002) Identification of a novel maturation mechanism and restricted substrate specificity for the SspB cysteine protease of *Staphylococcus aureus*, *J. Biol. Chem. 277*, 41770−41777.
22. McGahee, W., and Lowy, F. D. (2000) Staphylococcal infections in the intensive care unit, *Semin. Respir. Infect. 15*, 308−313.
23. Mori, S., Abeygunawardana, C., Johnson, M. O., and van Zijl, P. C. M. (1995) Improved senesitivity of HSQC spectra of exchanging protons at short interscan delays using a new fast HSQC (FHSQC) detection scheme that avoids water saturation, *J. Magn. Reson. B 108*, 94−98.
24. Muehlhahn, P., Bernhagen, J., Czisch, M., Georgescu, J., Renner, C., Ross, A., Bucala, R., and Holak, T. A. (1996) NMR characterization of structure, backbone dynamics, and glutathione binding of the human macrophage migration inhibitory factor (MIF), *Protein Sci. 5*, 2095−2103.
25. Novick, R. P. (2000) Pathogenicity factors and their regulation in *Gram-Positive Pathogens* (Fischetti, V. A., Novick, R. P., Ferretti, J. J., Portnoy, D. A., and Rood, J. I., Eds.) pp 392−407, American Society for Microbiology, Washington, DC.
26. Piotto, M., Saudek, V., and Sklenar, V. (1992) Gradient-Tailored excitation for single-quantum NMR spectroscopy of aqueous solutions, *J. Biomol. NMR 2*, 661−666.

27. Potempa, J., Dubin, A., Korzus, G., and Travis, J. (1988) Degradation of elastin by a cysteine proteinase form *Staphylococcus aureus*, *J. Biol. Chem. 263*, 2664−2667.
28. Read, R. J., and James, M. N. G. (1986) Introduction to the protein inhibitors: X-ray crystallography in *Proteinase inhibitors* (Barrett, A. J., and Salvesen, G., Eds.) pp 301−336, Elsevier, Amsterdam.
29. Rehm, T., Huber, R., and Holak, T. (2002) Application of NMR in structural proteomics: screening for proteins amenable to structural analysis, *Structure (Cambridge) 10*, 1613−1618.
30. Renner, C., Schlieicher, M., Moroder, L., and Holak, T. A. (2002) Practical aspects of the 2D ^{15}N-{^{1}H}-NOE experiment, *J. Biomol. NMR 23*, 23−33.
31. Rice, K., Peralta, R., Bast, D., Azavedo, J., and McGavin, M. J. (2001) Description of staphylococcus serine protease (*ssp*) operon in *Staphylococcus aureus* and nonpolar inactivation of *sspA*-encoded serine protease, *Infect. Immun. 69*, 159−169.
32. Ruoppolo, M., Freedman, R. B., Pucci, P., and Marino, G. (1996) Glutathione-dependent pathways of refolding of RNase T1 by oxidation and disupfide isomerization: catalysis by protein disulfide isomerase, *Biochemistry 35*, 13636−13646.
33. Rzychon, M., Filipek, R., Sabat, A., Kosowska, K., Dubin, A., Potempa, J., and Bochtler, M. (2003) Staphostatins resemble lipocalins, not cystatins in fold, *Protein Sci. 12*, 2252−2256.
34. Rzychon, M., Sabat, A., Kosowska, K., Potempa, J., and Dubin, A. (2003) Staphostatins: an expanding new group of proteinase inhibitors with a unique specificity for the regulation of staphopains, *Staphylococcus* spp. cysteine proteinases, *Mol. Microbiol. 49*, 1051−1066.
35. Sklenar, V., Piotto, M., Leppik, R., and Saudek, V. (1993) Gradient-Tailored Water Suppression for 1H-15N HSQC Experiments Optimized to Retain Full Sensitivity, *J. Magn. Reson. A 102*, 241−245.
36. Skelton, N. J., Palmer, A. G., Akke, M., Kordel, J., Rance, M., and Chazin, W. J. (1993) Practical Aspects of Two-Dimensional Proton-Detected ^{15}N Spin Relaxation Measurements, *J. Magn. Reson. B 102*, 253−264.
37. Stennicke, H. R., Ryan, C. A., and Salvesen, G. S. (2002) Reprieval from execution: the molecular basis of caspase inhibition, *Trends Biochem. Sci. 27*, 94−101.
38. Takahashi, M., Tezuka, T., and Katunuma, N. (1994) Inhibition of growth and cysteine proteinase activity of *Staphylococcus aureus* V8 by phosphorylated cystatin α in skin cornified envelope, *FEBS Lett. 355*, 275−278.
39. Travis J., Potempa J., and Maeda, H. (1995) Are bacterial proteinases pathogenic factors?, *Trends Microbiol. 3*, 405−407.
40. Varadi, D. P., and Saqueton, A. C. (1968) Elastase form *Staphylococcus epidermidis*, *Nature 218*, 468−470.
41. Vuister, G. W., and Bax, A. (1993) Quantitative J correlation−a new approach for measuring homonuclear 3-bond J (H(N)H(α)) coupling constants in ^{15}N-enriched proteins, *J. Am. Chem. Soc. 115*, 7772−7777.
42. Wüthrich, K. (1986) *NMR of Proteins and Nucleic Acids*, John Wiley, New York.
43. Zweckstetter, M., and Holak, T. A. (1999) Robust refocusing of 13C magnetization in multidimensional NMR experiments by adiabatic passage pulses, *J. Biomol. NMR 15*, 331−334.

BI035310J